Hydrol. Earth Syst. Sci. Discuss.,
https://doi.org/10.5194/hess-2020-633-AC2, 2021

Hydrology and Earth System Sciences
Discussions

Interactive comment on "Rainfall erosivity estimation using gridded daily precipitation datasets" *by* Maoqing Wang et al.

Maoqing Wang et al.

201921051015@mail.bnu.edu.cn

Received and published: 5 March 2021

Please see attached .pdf supplement for response to RC2. Reviewer comments have been copied in black font. Our responses are written in blue font. For the figures that are not clearly displayed in the manuscript, we have attached high-resolution images. Figure 7 and the captions of Figure 3, 4, 5 and 6 have been revised according to the comments.

Please also note the supplement to this comment:
https://hess.copernicus.org/preprints/hess-2020-633/hess-2020-633-AC2-supplement.pdf

Interactive comment on Hydrol. Earth Syst. Sci. Discuss., https://doi.org/10.5194/hess-2020-633, 2020.

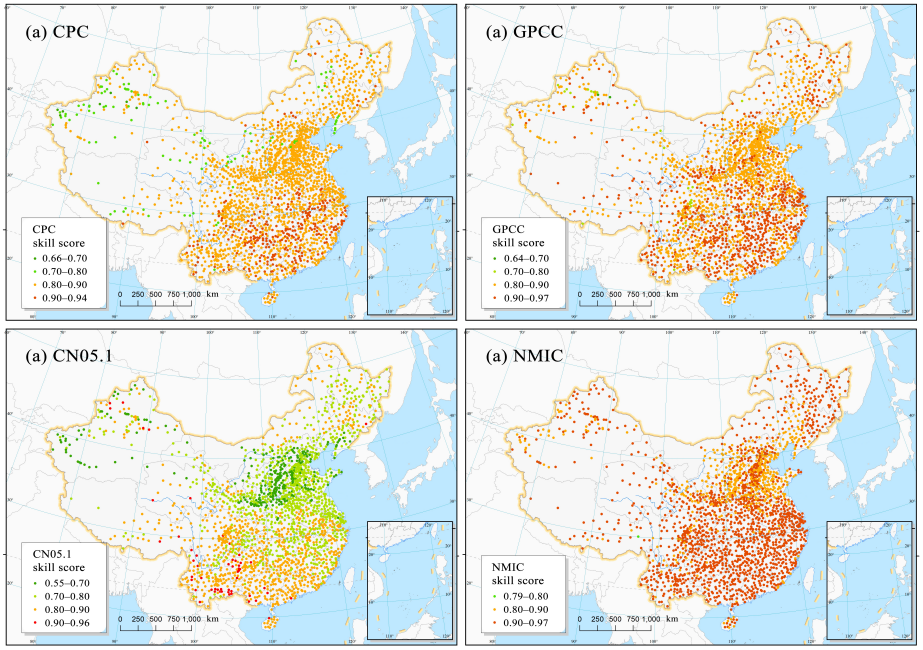

Figure 2. Spatial distributions of the skill scores for (a) CPC, (b) GPCC, (c) CN05.1, and (d) NMIC.

Fig. 1.

C3

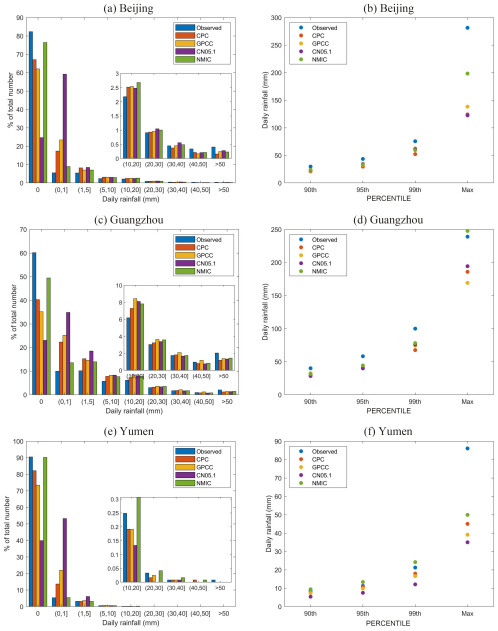

Figure 3. Comparison of the frequency distribution histograms of daily precipitation amounts and the extreme daily precipitation amounts between the gauge observations and four gridded datasets: (a) histogram, Beijing, (b) extreme daily precipitation amounts, Beijing, (c) histogram, Guangzhou, (d) extreme daily precipitation amounts, Guangzhou, (e) histogram, Yumen, and (f) extreme daily precipitation amounts, Yumen.

Fig. 2.

C4

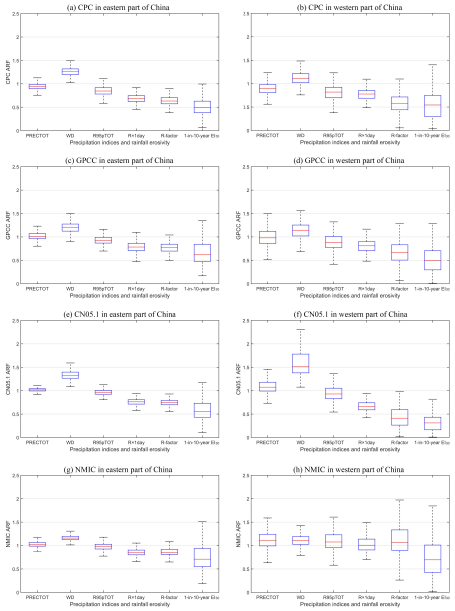

Figure 4. ***Ratios*** **for the precipitation metrics and rainfall erosivity values. The bars show the variation across the stations, marking the median, Q1 and Q3 ranges (box), and the whiskers mark the range of Q1 – 1.5IQRs to Q3 + 1.5IQRs (dashes):**
(a) CPC in the eastern part of China, (b) CPC in the western part of China, (c) GPCC in the eastern part of China, (d) GPCC in the western part of China, (e) CN05.1 in the eastern part of China, (f) CN05.1 in the western part of China, (g) NMIC in the eastern part of China, and (h) NMIC in the western part of China.

Fig. 3.

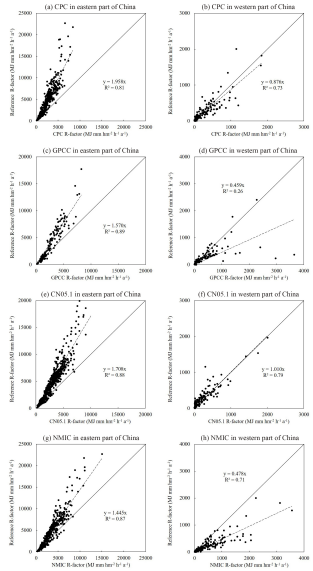

Figure 5. Comparison of the R-factors estimated from the gridded data and those extracted from Yue' s map. Due to the different spatial resolutions, the number of independent grid cells corresponding to stations used for the correction factor establishment in the four gridded datasets is different.
(a) CPC in the eastern part of China using 417 grid cells, (b) CPC in the western part of China using 149 grid cells, (c) GPCC in the eastern part of China using 163 grid cells, (d) GPCC in the western part of China using 126 grid cells, (e) CN05.1 in the eastern part of China using 587 grid cells, (f) CN05.1 in the western part of China using 158 grid cells, (g) NMIC in the eastern part of China using 416 grid cells, and (h) NMIC in the western part of China using 149 grid cells.

Fig. 4.

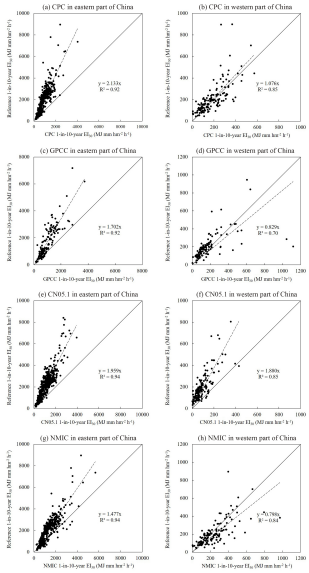

Figure 6. Comparison of the 1-in-10-year event EI_{30} estimated from the gridded data and those extracted from Yue' s map. Due to the different spatial resolutions, the number of independent grid cells corresponding to stations used for the correction factor establishment in the four gridded datasets is different.
(a) CPC in the eastern part of China using 417 grid cells, (b) CPC in the western part of China using 149 grid cells, (c) GPCC in the eastern part of China using 163 grid cells, (d) GPCC in the western part of China using 126 grid cells, (e) CN05.1 in the eastern part of China using 587 grid cells, (f) CN05.1 in the western part of China using 158 grid cells, (g) NMIC in the eastern part of China using 416 grid cells, and (h) NMIC in the western part of China using 149 grid cells.

Fig. 5.

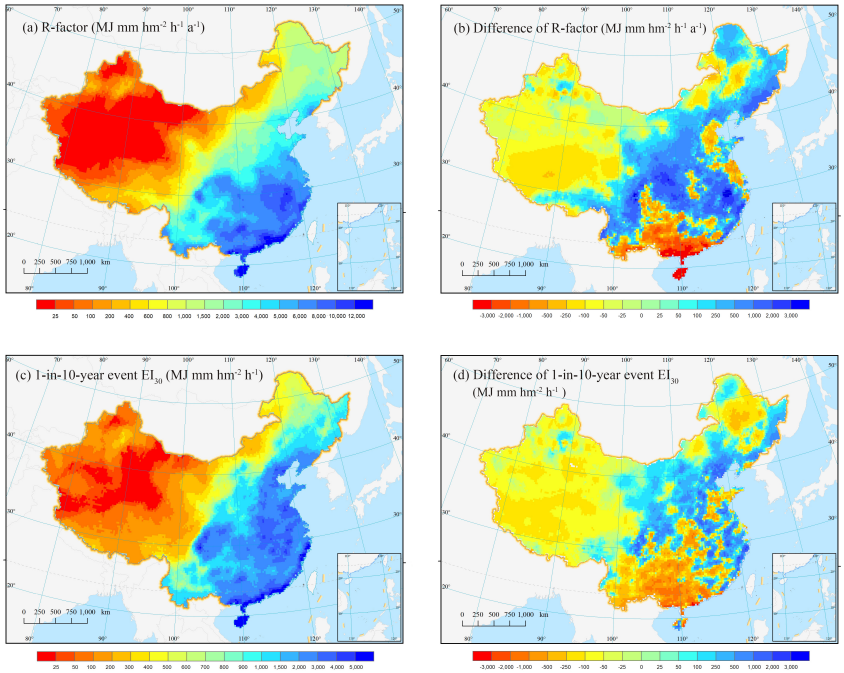

Figure 7. Spatial distribution of the R-factor and 1-in-10-year event EI30 using CN05.1 with bias correction factors (a and c), and the difference (b and d) in comparison with the original R-factor map (Yue et al., 2020b).

Fig. 6.